REVEALING AND MINIMIZING HIDDEN ENERGY LOSSES IN HYDRAULIC LINES OF MOBILE MACHINERY

by

***Ismail BOGREKCI*[a], *Pinar DEMIRCIOGLU*[a*], *E. Orcun KOZAKA*[a], *and Nuri UYSAL*[b]**

[a] Department of Mechanical Engineering, Faculty of Engineering, Aydin Adnan Menderes University, Aydin, Turkey
[b] R&D Center of EYS Company, Efeler, Aydin, Turkey

Original scientific paper
https://doi.org/10.2298/TSCI2504061B

In a mobile material handling system powered by hydraulic drives, abnormally high line pressures were observed during operation, raising concerns about energy losses and inefficiencies in the hydraulic circuit design. To quantify the actual power consumed by hydraulic motors vs. the power lost due to line friction, a comprehensive measurement and simulation study was conducted. Pressure sensors (minimes test points) were installed at the inlet and outlet of each hydraulic motor to collect real-time pressure data. Losses were categorized into two main components: internal motor losses and line friction losses. An Excel-based tool was developed to calculate power losses [kW], and a MATLAB SIMULINK model was constructed to simulate pressure drops across the system, including components such as elbows, reducers, and fittings. Results indicated that frictional losses in the hydraulic lines accounted for nearly 50% of the total power drawn by the motors. Although the original line design adhered to standard velocity-based guidelines, Reynolds number analysis revealed a transitional to turbulent flow regime, contributing significantly to energy loss. Simulation of different internal diameters demonstrated that increasing the line size from 1/2"-5/8" in a critical segment reduced the associated power loss from 4-0.8 kW – a reduction of over 80%. Overall, approximately 7 kW of hydraulic power was recovered from a 55 kW engine, enabling the redirection of surplus energy to auxiliary hydraulic functions and improving overall fuel efficiency.

Key words: *hydraulic line losses, pressure drop, SIMULINK modeling, energy recovery, Reynolds number, mobile machinery*

Introduction

Hydraulic systems are omnipresent in today's mobile equipment, with benefits that include high power density, compact structure, and better control precision. However, in spite of these advantages, the overall performance of hydraulic systems is significantly influenced by internal fluid dynamics, especially in structures with large and complicated piping systems. Energy losses caused by internal friction, turbulence, and geometric constraints (*e.g.*, tight elbows and T-junctions) can considerably decrease energy efficiency and lead to a higher system load. This paper examines a prototype mobile screening unit employed in aggregate processing and mining operations, which utilizes a hydraulic drive system to operate various

* Corresponding author, e-mail: pinar.demircioglu@adu.edu.tr

conveyor belts. Although the hydraulic motors in this system were within their specified operation, abnormally high system pressures were discovered during routine operational testing. The elevated pressures were not in accordance with the mechanical load being applied to the motors, reflecting substantial energy losses occurring in the hydraulic transmission lines. Interestingly, the hydraulic design had initially been engineered to meet standard requirements outlined in the Hydraulic Piping Standards Handbook, though due to the overall length of the lines and minuscule internal diameters of a number of crucial components, the system warranted closer scrutiny.

The preliminary tests were carried out under summer conditions (July), whereby pressure losses remained within acceptable limits, hence rendering additional research moot. However, subsequent testing under winter conditions (January) with ISO VG 46 hydraulic fluid registered a noteworthy rise in system pressure and energy consumption. A basic experimental apparatus was therefore devised for measuring the power absorbed by hydraulic motors through direct measurement techniques and bypassing methods under different temperature conditions. In order to obtain a more in-depth understanding of the system dynamics and establish possible sources of inefficiency, a simulation model in MATLAB/SIMULINK was set up. The model accurately mirrored the hydraulic circuit of the prototype, line geometries, and operating torques, thereby enabling in-depth examination of the influence of line diameter on pressure losses and power consumption. Simulation outcomes indicated that the enlargement of the internal diameter of critical pipe sections from 1/2" (12 mm) to 5/8" (16 mm) resulted in a considerable decrease in pressure losses. In a critical section, the power loss that was calculated fell from 4-0.8 kW, an 80% reduction.

About 7 kW of hydraulic power was recovered from the system, thereby increasing the functional efficiency of the 55 kW Diesel engine and facilitating the diversion of surplus energy to auxiliary operations or fuel efficiency enhancement. This study demonstrates the merit of combining empirical measurement and optimization using simulations in identifying and addressing latent inefficiencies in hydraulic systems. Of particular importance, the gains were realized without redesign or replacement of hardware, indicating that diligent system-level analysis. Especially of network configuration and line sizing, can greatly improve energy efficiency in mobile hydraulic equipment operating under time-varying environmental conditions.

Literature review

Hydraulic fluid power systems transform mechanical energy into hydraulic energy in order to generate, control, and transfer power via actuators. Due to their high power density, precision, and reliability, hydraulic fluid power systems find extensive applications in transportation, construction, robotics, agricultural, and oil and gas markets. Their capacity to endure severe environments and their ruggedness suit them for continuous-duty applications. In addition, hydraulic systems transmit power effectively over long distances and are, therefore, ideally suited for applications where actuators are far away from the power source. Their durability and efficiency are the reasons for increased productivity, precision, and operational flexibility in a very large number of industrial applications [1-3].

Energy losses in hydraulic systems, especially those caused by line components like fittings, bends, and pipeline geometry, are of prime concern in aircraft and mobile hydraulic systems. Hydraulic line energy losses are a crucial factor in mobile and stationary hydraulic systems. They have a direct effect on system efficiency, fuel consumption, and mechanical output power availability. Distributed losses caused by fluid friction along the pipe wall and local losses caused by fittings, bends, valves, and other constrictions are the two major sources of energy loss in hydraulic pipes [4]. In a succession of experiments, it has been time and again established that pressure drops, operating time lags, and power consumption are the results of local resistances caused by angular fittings or misaligned hoses.

Traditional design practice, *i.e.*, ISO 4413 and industry standards (*e.g.*, Rexroth or SAE), tends to be based on recommended flow velocities (*e.g.*, 2-6 m/s for pressure lines) as a pipe sizing requirement [5]. Easy to use for initial design, such practices do not incorporate flow regime change fully. When Reynolds number is greater than ~4000, the flow is turbulent and losses are significantly heightened by the formation of eddies and stochastic velocity profiles [6].

Valdes *et al.* [7] proposed a parameterization method for flow and resistance coefficients of hydraulic fittings, summoning empirical models for different connection geometries. Complementing this, De Moraes *et al.* [8] experimentally determined head loss coefficients for a number of fittings, showing that classical approximations consistently underestimate the real losses, especially for turbulent flow regimes.

Li *et al.* [9] presented a review of state-of-the-art modeling techniques for transient hydraulic behavior analysis with a focus on the use of CFD for the modeling of time-dependent flow processes in fitting-dominated circuits. In the same way, Liu *et al.* [10] illustrated that even small minimizations of pressure loss can notably reduce energy consumption and enhance actuator responsiveness in hydraulic power units.

More recent research by Chuang and Ferng [11] was concerned with thermal-hydraulic performance in T-junctions, demonstrating that flow velocity variation and injection angle significantly affect turbulence, thereby increasing energy losses. This is consistent with the research by Yan *et al.*, [12] who created energy conservation strategies for hydraulic presses through dynamic flow rate control and minimization of excess pressure losses.

In application-specific aerospace research, Zhang *et al.* [13] analyzed the actuation delay in electro-hydrostatic actuators, demonstrating that small discrepancies in flow performance through fitting design can create significant timing inefficiencies in control systems. Stosiak [14] also modeled the dynamic behavior of the hydraulic distributor, commenting that interactions between slides and sleeves have the potential to increase resistance under alternating pressure conditions.

Hydraulic line energy losses are not only passive inefficiencies but also active constraints on system responsiveness, precision, and efficiency. To enhance them is to transcend velocity-based sizing rules to integrated approaches encompassing real-time data acquisition, flow modeling, and iterative design. The developing convergence of empirical measurement, simulation environments, and digital twin concepts is an encouraging trajectory toward smarter, more energy-efficient hydraulic architectures for stationary and mobile systems.

Material and methodology

System configuration

This study focuses on both the experimental and simulation analysis of high line losses that occur at low temperatures during the testing of energy losses in the hydraulic drive system of a mobile screening station, which is commonly used in the aggregate processing and mining sectors. The system includes fixed displacement hydraulic motors that drive various conveyor belts. Hydraulic power is supplied by two gear pumps driven by a Diesel engine operating at 2000 rpm. One pump has a displacement of 20 cm^3 per rev, and the other 16 cm^3 per rev, each supplying hydraulic power to specific groups of belts.

The 20 cm^3 pump is connected in series to two belts: the cross belt and the side belt. This line is then connected to a side port of a T-junction (T1). The 16 cm^3 pump is connected in series to the underscreen belt and the rear belt, and this flow is directed to a different T-junction (T2). The inner diameter of the pipe line between T1, T2, and the final T-junction is 24 mm. This configuration is also reflected in the system model. The pipe length between each pump and hydraulic motor, and between the T-junctions, ranges from approximately 8 m to 12 m, with hydraulic hoses having an inner diameter of 12 mm. Since the elbows are galvanized, a surface roughness value of 150 µm is used. The elbows used have an inner diameter of 10 mm and a bend radius of 12 mm, and these values are incorporated into the model. With an increase in pipe diameter, the elbow diameter becomes 16 mm with an 18 mm bend radius. Surface roughness remains unchanged. The hydraulic motors, pressure relief valves, and pumps are sourced from MATLAB Parker library and are equivalent to the physical pumps used in the system. Conveyor belts will not be detailed in the simulation. Only simulation data relevant to examining the viscosity of ISO VG 46 oil at low temperatures will be shared. In the first case, the pipe diameter is 1/2", corresponding to an inner diameter of 12 mm. When increased to 5/8", the inner diameter becomes 16 mm. The actual field image showing the overall layout of the system and the conveyor belt groups is presented in fig. 1, while the hydraulic circuit diagram and the Simulink model are provided in detail in fig. 2. In tab. 1 the line design parameters are presented.

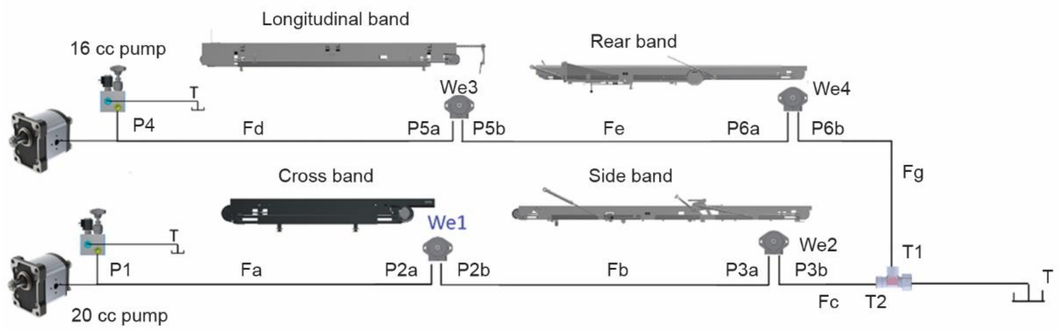

Figure 1. Line diagram

The flow rates and velocities for the line design were calculated. For the 16 cc pump, a flow rate of 32 Lpm and an inner diameter of 12 mm:

$$v = \frac{Q}{A} = \frac{0.000533 \text{ m}^3/\text{s}}{1.131 \cdot 10^{-4} \text{ m}^2} = 4.71 \text{ m/s}$$

and for the 20 cc pump, a flow rate of 40 Lpm and an inner diameter of 12 mm:

$$v = \frac{Q}{A} = \frac{0.0006667 \text{ m}^3/\text{s}}{1.131 \cdot 10^{-4} \text{ m}^2} = 5.89 \text{ m/s}$$

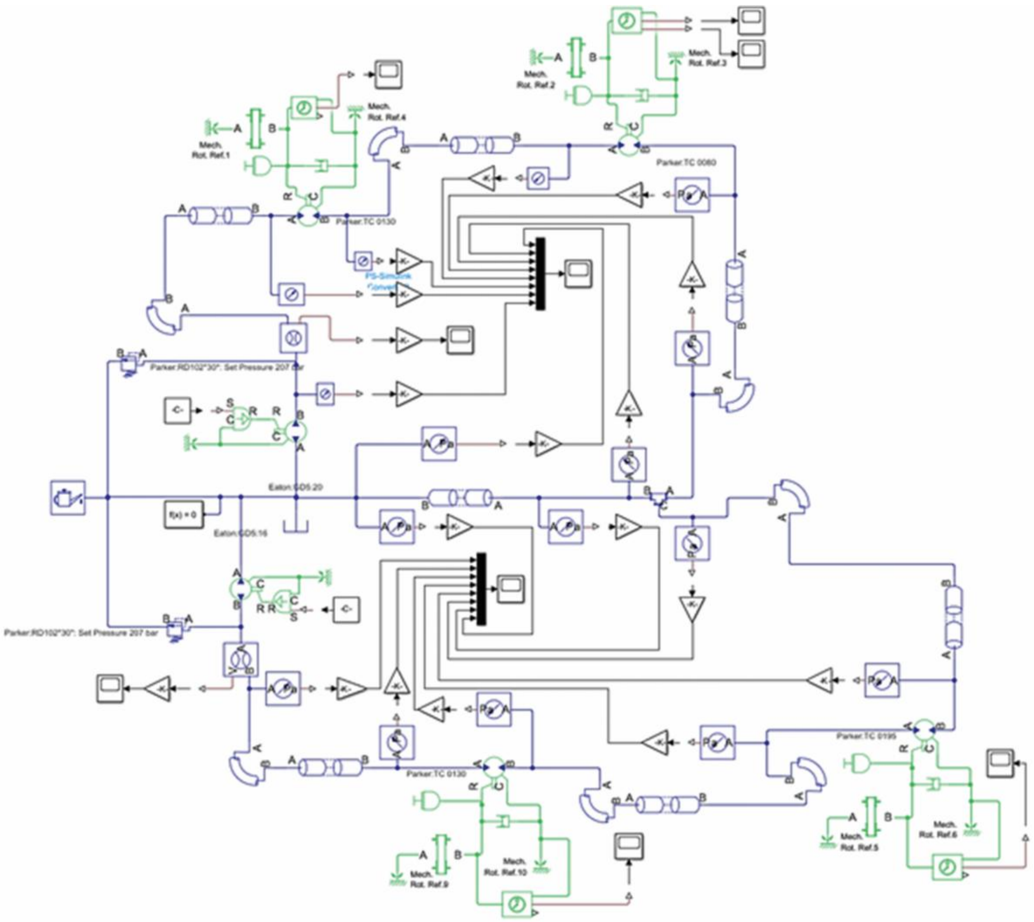

Figure 2. The MATLAB SIMULINK circuit diagram

Table 1. Line design parameters (Gs hydro)

Region of the pipeline	Recommended flow velocity, *v* [ms^{-1}]	Maximum allowed flow velocity, *v* [ms^{-1}]
Suction line	0.5-1.0	1.0-1.5
Return line	1.0-3.0	3.0-4.0
Pressure line 6.3-10 MPa	4.0-4.5	6.0
Pressure line 10-16 MPa	4.5-5.0	6.0
Pressure line 16-25 MPa	5.0-5.5	6.0
Pressure line 25-40 MPa	5.5-6.0	6.0

Minimes devices and measurement lines

To evaluate energy losses within the hydraulic lines, minimes devices were strategically installed at the inlet and outlet of the hydraulic motors. This instrumentation enabled the precise determination of parameters such as the power [kW] drawn by the hydraulic motors from the system, as well as the associated line losses. In order to validate the measured line losses, a secondary measurement was conducted wherein the hydraulic motors were bypassed. Pressure readings were acquired using standard pressure transmitters and calibrated manometers. All measured data were systematically recorded and compiled for reporting and analysis purposes. Figure 3 shows minimes devices used for pressure measurements with and without hydraulic motor bypass.

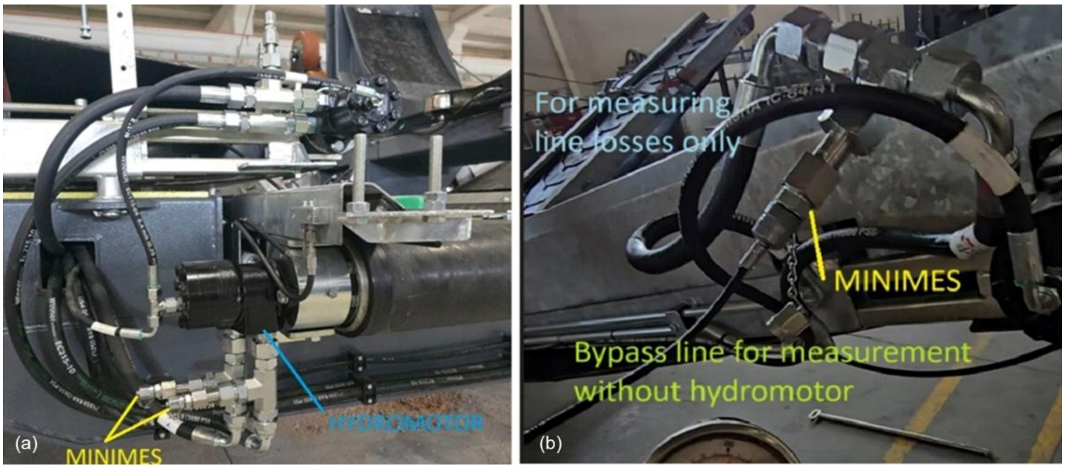

Figure 3. Minimes devices used for measuring the inlet and outlet pressures of the hydraulic motor (a), and minimes devices used for pressure measurement with the hydraulic motors bypassed (b)

Measurement of system pressures and discussion of the values

To test the prototype under winter conditions, a short test was conducted by operating the machine at an ambient temperature of approximately 15 °C. The objective was to evaluate the pressure values at the pump outlet. During the test, high pressure readings were observed at the outlets of two pumps. To determine how much energy the hydraulic motors were drawing from the system, measurements were carried out using minimes devices at approximately 15 °C. Based on these measurements, the tables below were generated. The initial focus of the test was on quantifying the energy drawn from the line by the hydraulic motors We1, We2, We3, and We4. Additionally, energy losses in the lines due to turbulence and other factors; represented by the values Fa, Fb, Fc, Fd, Fe, and Fg, were calculated using the measured pressure data.

Since the line values in tab. 2 were considered too high to be solely attributed to hydraulic motor consumption, a second test was conducted by bypassing the hydraulic motors, as shown in the set-up in section *Minimes devices and measurement lines*. The goal was to isolate and measure only the line losses. Based on this configuration, tab. 3 was generated. As observed, even when no part of the system was operating, line losses of 4.9 kW and 1.8 kW were recorded, values surprisingly close to those seen when the hydraulic motors were active. When the system temperature was increased to 45 °C, these losses approached approximately 7 kW. Considering that a radiator is also employed to cool the system, this energy loss becomes even more significant. Due to the strong temperature dependency of these losses and in order to observe system behavior at lower temperatures, it was decided to develop a model in MATLAB SIMULINK to better estimate optimal operating conditions. While modeling the system in Simulink, parameters such as pipe diameters and surface roughness values were also included.

Table 2. Measurement results with hydraulic motors

TEST DATA WITH HYDROMOTOR(15c°)

	MODE	P1(bar)	P2a	P2b	P3a	P3b		MODE	P4	P5a	P5b	P6a	P6b
20cc PUMP	Idle mode(900rpm)	94	85	40	28	10	16cc PUMP	Idle mode(900rpm)	61	55	35	34	5
	Eco mode(1600 rpm)	140	120	65	45	20		Eco mode(1600 rpm)	83	70	47	45	10
	Power mode(2000 rpm)	166	145	80	55	27		Power mode(2000 rpm)	95	80	54	50	14

Pressure losses (given in bar)

	MODE	Debi(lt)	Fa	Fb	Fc		FLOW(lt)	Fd	Fe	Fg		We1	We2	We3	We4
20cc PUMP	Idle mode(900rpm)	18	9	12	10	16cc PUMP	14,4	6	1	5	Hidromotorlar	45	18	20	29
	Eco mode(1600 rpm)	32	20	20	20		25,6	13	2	10		55	25	23	35
	Power mode(2000 rpm)	40	21	25	27		32	15	4	14		65	28	26	36

Losses(Kw)

	MODE	Debi(lt)	Fa	Fb	Fc		FLOW(lt)	Fd	Fe	Fg		We1	We2	We3	We4		We1+We2	Fa+Fb+Fc	Çapraz+yan	We3+We4	Fd+Fe+Fg	Elek+arka
20cc PUMP	Idle mode(900rpm)	18	0,27	0,36	0,3	16cc PUMP	19,8	0,144	0,024	0,12	Hidromotorlar	1,08	0,432	0,48	0,696	Toplam KW	1,512	0,93	2,442	1,176	0,288	1,464
	Eco mode(1600 rpm)	32	1,06667	1,066667	1,066667		35,2	0,554667	0,085333	0,426666667		2,346667	1,066667	0,981333	1,493333		3,413333	3,2	6,613333	2,4746667	1,066667	3,54133333
	Power mode(2000 rpm)	40	1,4	1,666667	1,8		44	0,8	0,213333	0,746666667		3,466667	1,493333	1,386667	1,92		4,96	4,866667	9,826667	3,3066667	1,76	5,06666667
																			Hat kaybı%			Hat kaybı%
																			38,08354			19,6721311
																			48,3871			30,1204819
																			49,5251			34,7368421

Table 3. Measurement results with hydraulic motors bypassed

TEST DATA WITHOUT HYDROMOTOR (15C°)

	Güç modu	P1(bar)	P2	P3		P4	P5	P6
20cc PUMP	Idle mode(900rpm)	31,3	24	13	16cc PUMP	15,6	12	7
	Eco mode(1600 rpm)	64,2	48	25		31,5	22	13
	Power mode(2000 rpm)	84	62	32		41	28	17

Pressure losses (given in bar)

	Güç modu	Debi(lt)	Fa	Fb	Fc		Debi(lt)	Fd	Fe	Fg		We1	We2	We3	We4
20cc PUMP	Idle mode(900rpm)	18	7,3	11	13	16cc PUMP	14,4	3,6	5	7	Hidromotors (Approximately)	45	18	20	29
	Eco mode(1600 rpm)	32	16,2	23	25		25,6	9,5	9	13		55	25	23	35
	Power mode(2000 rpm)	40	22	30	32		32	13	11	17		65	28	26	36

Losses(Kw)

	Güç modu	Debi(lt)	Fa	Fb	Fc		Debi(lt)	Fd	Fe	Fg		We1	We2	We3	We4		We1+We2	Fa+Fb+Fc	Çapraz+yan	We3+We4	Fd+Fe+Fg	Elek+arka
20cc PUMP	Idle mode(900rpm)	18	0,219	0,33	0,39	16cc PUMP	14,4	0,0864	0,12	0,168	Hidromotors (Approximately)	1,35	0,54	0,48	0,696	Toplam KW	1,89	0,939	2,829	1,176	0,3744	1,5504
	Eco mode(1600 rpm)	32	0,864	1,226667	1,333333		25,6	0,405333	0,384	0,554666667		2,933333	1,333333	0,981333	1,493333		4,266667	3,424	7,690667	2,4746667	1,344	3,81866667
	Power mode(2000 rpm)	40	1,46667	2	2,133333		32	0,693333	0,586667	0,906666667		4,333333	1,866667	1,386667	1,92		6,2	5,6	11,8	3,3066667	2,186667	5,49333333
																			Hat kaybı%			Hat kaybı%
																			33,19194			24,1486068
																			44,5215			35,1955307
																			47,45763			39,8058252

The MATLAB SIMULINK tables and values

The MATLAB general schema values

Figure 4 was designed to measure line losses using only the bypass line, without hydraulic motors. Line losses will be measured from this set-up. This configuration allows for the isolation and direct measurement of line-induced energy losses.

The MATLAB pipe bend value

In the simulation model, the pipe bend (IL) block was configured to realistically represent the geometry and material characteristics of the hydraulic lines used in the actual system. The pipe diameter was set to 10 mm, and the bend radius was defined as 12 mm to match the physical fittings present in the hydraulic circuit. A bend angle of 90° was applied to accurately model the common elbow connections found in the system. The internal surface absolute roughness was set to $1.5 \cdot 10^{-4}$ m (150 µm). This relatively high roughness value reflects the condition of galvanized fittings, which typically exhibit greater surface irregularities compared to smooth rubber hoses. Such fittings, especially when aged or subjected to industrial environments, can develop internal corrosion or manufacturing defects that increase flow resistance, thereby justifying the use of this roughness value in the model.

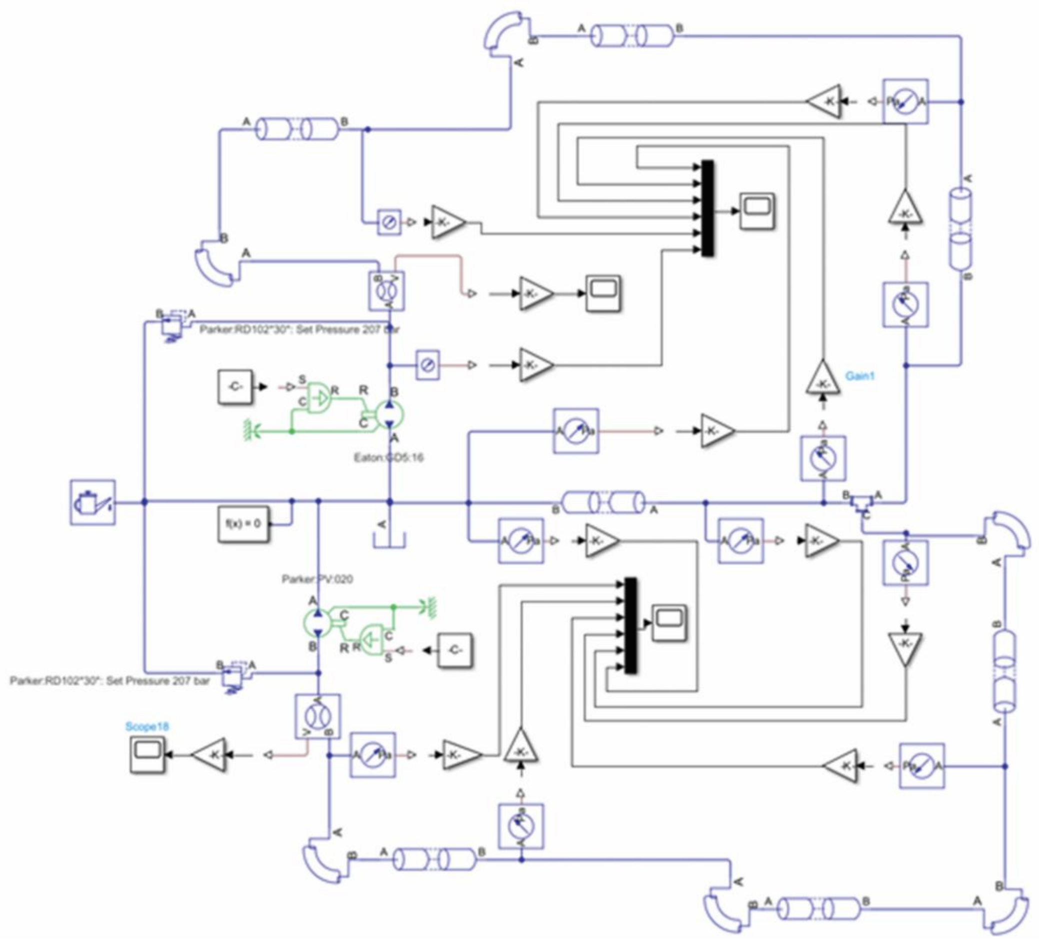

Figure 4. Simulink model of the lines

The fluid dynamic compressibility option was disabled, as the focus of this simulation is on low-pressure return and suction lines. In these sections of the hydraulic system, compressibility effects are minimal and do not significantly impact flow behavior. Therefore, ignoring fluid compressibility is a valid simplification for the scope of this study.

The MATLAB pipe (IL)

To accurately simulate the energy losses in the hydraulic lines, the pipe (IL) block in MATLAB SIMULINK was configured with values derived from actual system geometry and empirical data. Each parameter was carefully selected as follows.

In the simulation environment, the pipe (IL) block was configured to accurately represent the hydraulic hose geometry and flow conditions of the real system. A total of six pipes with an inner diameter of 12 mm were modeled to represent the main hydraulic lines. In addition, one pipe with a 24 mm inner diameter was included to represent the suction line. The pipes were discrete based on actual routing lengths: three of the pipes were modeled with a length of 10 m, while the remaining four pipes were modeled with a length of 8 m. The total layout reflects the physical distribution of hydraulic lines in the system.

An elevation gain of 1 m was introduced to account for minor gravitational effects due to the vertical positioning of components, using the standard gravitational constant of 9.81 m/s². Viscous friction losses were calculated using the Haaland correlation, which is suitable for both laminar and turbulent flow conditions. Local resistances such as elbows and T-junctions were represented by an equivalent straight-pipe length of 1 m. The internal surface roughness was defined as 0.03 mm, consistent with values typical for new rubber hoses. Flow regime thresholds were set based on the Reynolds number, with 2000 as the laminar limit and 4000 as the onset of turbulent flow. The pipe wall was assumed rigid, and the initial fluid pressure was taken as atmospheric (0.101325 bar). This configuration enabled the model to replicate realistic flow behavior, and the results were validated through comparison with experimental measurements.

The MATLAB T-junction (IL)

The T-Junction (IL) block was configured to accurately represent the flow splits and merges within the hydraulic system. The main and side branch areas were both set based on a hose with a 12 mm inner diameter, consistent with the actual components used in the physical set-up. This ensures that the simulated flow distribution and associated losses reflect real-world behavior. The Crane correlation was selected as the loss coefficient model. This empirical method is widely used to estimate local pressure losses in fittings like T-junctions and elbows, and is well-suited for both laminar and turbulent flow conditions. Its inclusion provides more realistic modeling of energy dissipation at junction points. A critical Reynolds number of 2000 was specified to define the transition between laminar and turbulent flow. This standard threshold helps the model correctly classify the flow regime during simulation, particularly under varying operating conditions.

In terms of configurability, the flow areas were set to be run-time configurable, allowing for testing or tuning during simulation, while the Reynolds number was kept compile-time fixed, as it is a physical property that does not change during execution. For initial conditions, the mass flow rates at ports A, B, and C were all set to 0 kg/s, with high priority assigned to ensure a stable and balanced starting point for the simulation. Overall, this configuration allows the T-junction to realistically reproduce the flow behavior and pressure distribution observed in the actual hydraulic system.

Isothermal liquid properties (IL)

The the isothermal liquid properties (IL) block was carefully configured to represent the real hydraulic oil characteristics used in the system. The density was set to 870 kg/m³, which corresponds to the typical density of mineral-based ISO VG 46 hydraulic oils. The isothermal bulk modulus was modeled as a constant value of $1.4 \cdot 10^9$ Pa, representing the compressibility behavior of hydraulic oil under normal operating pressures. This ensures that the simulation correctly reflects pressure wave propagation and system responsiveness.

The kinematic viscosity was set to 200 cSt, which corresponds to the viscosity of ISO VG 46 hydraulic oil at approximately 15 °C. This temperature-specific viscosity value was intentionally chosen because the hydraulic system in the simulation is expected to operate in environments where fluid temperature could be close to this value during cold start or low ambient temperature conditions. Using this value allows the model to account for the higher flow resistance and pressure drops typically seen when the oil is more viscous at lower temperatures.

The atmospheric pressure was set at 1 bar, and the minimum valid pressure was specified as 0.01 bar, to prevent unphysical negative pressures that could indicate cavitation risk or numerical instability. A warning is issued if this threshold is violated during the simulation.

In the entrained air section, a volumetric fraction of 0.005 was defined, indicating a 0.5% presence of entrained air, which is typical in hydraulic systems due to microscopic air bubbles or dissolved gas content. The air polytropic index was set to 1.0, assuming isothermal conditions for the trapped air, and the air density was defined as 1.225 kg/m^3, representing standard atmospheric conditions. The air dissolution model was deactivated for simplicity, as the simulation focuses on macroscopic fluid behavior rather than gas-liquid phase interactions.

With this set-up, the hydraulic fluid properties accurately represent the behavior of ISO VG 46 oil at 15 °C, ensuring realistic simulation of pressure losses, flow resistances, and dynamic system response under such thermal conditions.

Results and discussion

The scope data obtained from the line loss model designed in MATLAB SIMULINK exhibits a structure similar to the test data presented. During this process, improvements were made not only by increasing the pipe diameter, but also by reducing the number of elbow fittings. Additionally, a reduction in pressure drop was achieved by increasing the pipe diameter in the T-Junction (IL) section. The expected values were displayed on the screen accordingly.

Comparison of MATLAB SIMULINK model results with test data

The values simulated in MATLAB were calculated based on an operating speed of 2000 rpm. When compared with measurements taken during the hydraulic motor bypass tests, the simulated values align well with the test data. Although the Simulink results are slightly higher, a pressure value of 92 bar was observed. This deviation is believed to be caused by a reduction in viscosity due to localized heating. Similarly, the pressure for the 16 cc pump was measured at 53 bar. Based on these results, the Simulink model is considered to be valid. Building on this, we will proceed to evaluate line losses at 0 °C, again using an internal pipe diameter of 12 mm as the basis for analysis, fig. 5.

Evaluation of system pressure results in SIMULINK at 0 °C with a hose inner diameter of 12 mm

Since testing the prototype under 0 °C conditions in Aydin is not practically feasible, the evaluation will be conducted using the validated SIMULINK model we developed. The results obtained from the simulation will then be analyzed and interpreted accordingly.

Considering the presented results and the fact that the hydraulic motors operate at pressures exceeding 207 bar, it is evident that the system would be unable to provide the required flow rate to run the motors at full capacity. As a result, oil would be redirected to the tank via the pressure control valve, leading to energy losses. To mitigate this issue, it was anticipated that increasing the diameter of the T-Junction (IL) would help reduce the pressure drop. In the updated Simulink model, the T-junction diameter was increased to 25 mm, and the hose inner diameters were enlarged to 16 mm. The simulation results for this configuration at 15 °C are presented, fig. 6.

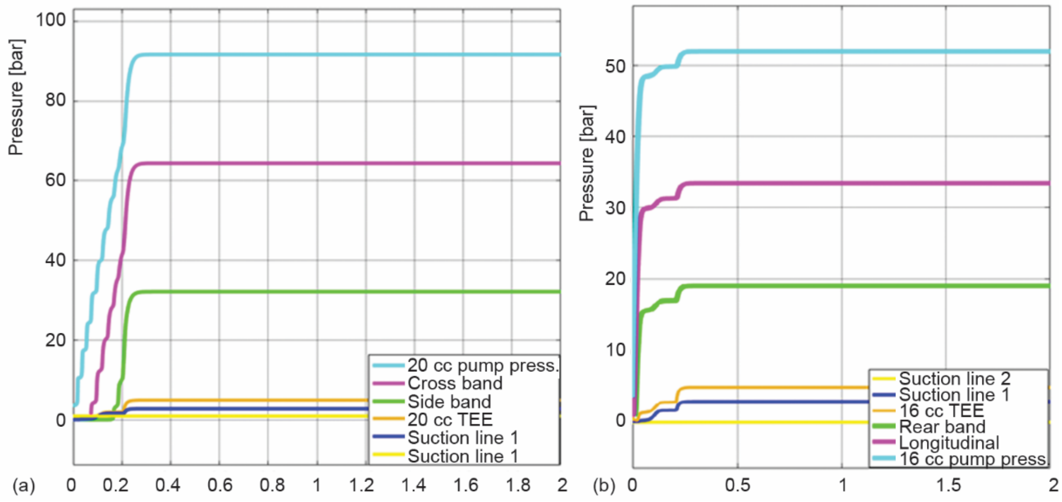

Figure 5. Pressure distribution across hydraulic circuit components for a 20 cc pump (a) and a 16 cc pump (b) at 15 °C (200 cSt viscosity) using Ø12 mm pipe inner diameter

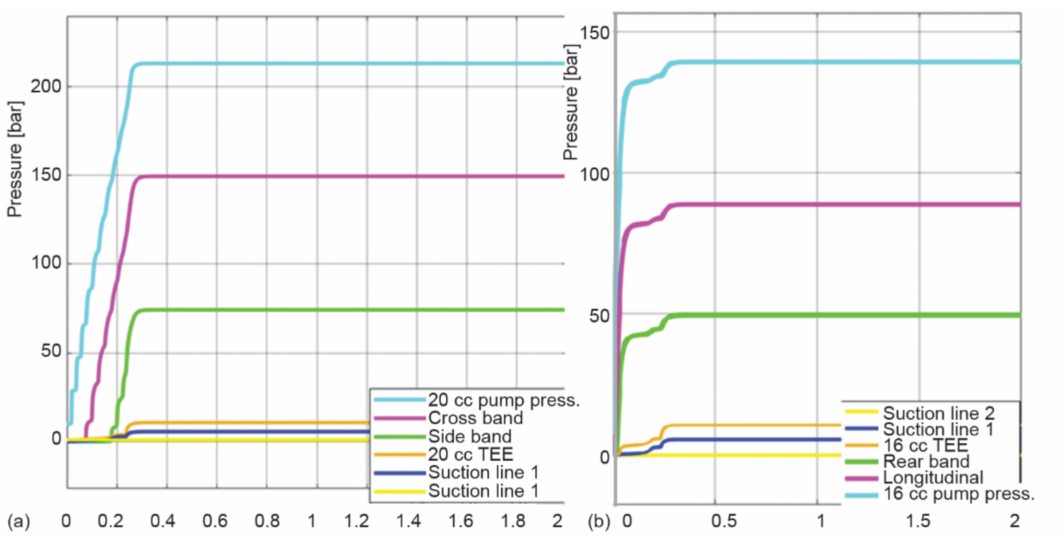

Figure 6. Pressure distribution across hydraulic circuit components for a 20 cc pump (a) and a 16 cc pump (b) at 0 °C (550 cSt viscosity) using Ø12 mm pipe inner diameter

Evaluation of system pressure results in SIMULINK at 15 °C with a hose inner diameter of 16 mm

At 15 °C in the SIMULINK model, the hose inner diameters were increased from 12 mm to 16 mm (5/8"), the elbow diameters were set to 16 mm with a bend radius of 18 mm, and the T-Junction (IL) diameter was increased from 12 mm to 25 mm. After implementing these modifications, the simulation produced the results are shown.

Increasing the pipe diameter to 16 mm at 15 °C resulted in a reduction of the pressure in the 20 cc pump from 92 bar to 26 bar. Similarly, in the 16 cc pump, the pressure dropped from 53 bar to 18 bar. Furthermore, increasing the diameters of the T-junction and elbow components in the system also contributed to the observed decrease in pressure values, as confirmed by the simulation results, fig. 7.

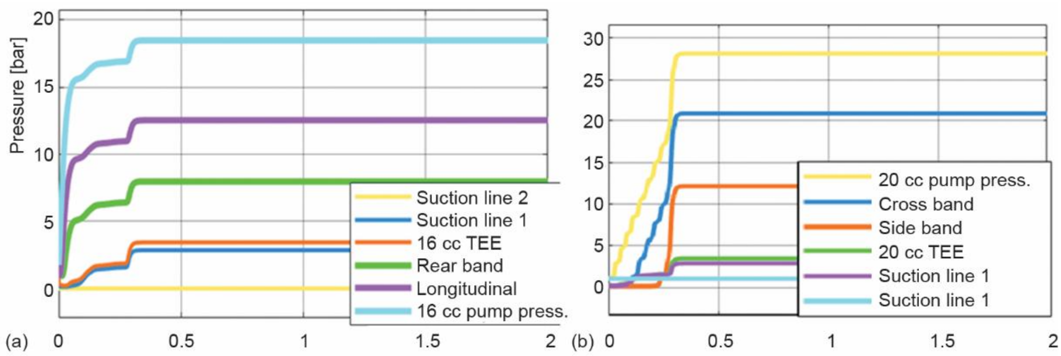

Figure 7. Pressure distribution across hydraulic circuit components for a 16 cc pump (a) and a 20 cc pump (b) at 15 °C (200 cSt viscosity) using Ø16 mm pipe inner diameter

Diameter optimization

During the field tests of the prototype hydraulic system, it was observed that even under continuous operation at an ambient temperature of approximately 15 °C, the fluid temperature within the hydraulic lines did not exceed 40 °C. This relatively low thermal rise is attributed to the extended length of the hydraulic lines and cold ambient conditions, both of which contributed to limited heat generation within the system.

As a result, the ISO VG 46 hydraulic oil retained a high viscosity throughout the test cycle. This elevated viscosity increased frictional losses, particularly in undersized hoses and fittings. Therefore, it became essential to optimize the internal diameters of the hydraulic lines, not solely based on nominal flow velocity guidelines, but also by accounting for actual operating viscosity under low-temperature conditions.

To evaluate this, a MATLAB Simulink model was developed to simulate the effects of increasing the internal diameter of the hydraulic lines from 1/2" (12 mm) to 5/8" (16 mm). The simulation revealed a significant reduction in power losses in critical sections of the system – specifically, a decrease from 4-0.8 kW in one of the most loss-prone segments. Across the entire hydraulic network, this adjustment led to an estimated energy recovery of 6 kW from the 55 kW Diesel engine.

These findings demonstrate that in hydraulic systems intended for cold climates or winter operation, the oil viscosity can remain high enough to cause substantial energy losses unless geometric optimizations are implemented. Hence, increasing the hose diameter was not only a performance-enhancing measure, but also a design necessity to maintain system efficiency and operability under extended low-temperature conditions.

In summary, this study underscores the sensitivity of hydraulic system efficiency to line diameter, particularly in applications where fluid temperatures remain low and thermal thinning of the oil is minimal during operation.

Discussion

This study demonstrates that standard hydraulic design guidelines, though widely adopted in industry, may fall short when addressing practical inefficiencies encountered under real-world operating conditions. Through a combination of empirical field measurements and MATLAB SIMULINK simulations, it was revealed that several sections of the hydraulic circuit operated within transitional to turbulent flow regimes, with Reynolds numbers ranging from 2300 to 4000. This flow behavior resulted in frictional energy losses significantly greater than those predicted by conventional, velocity-based sizing practices.

The primary factors contributing to these excessive losses included:
– small internal diameters of the hydraulic lines,
– a high number of elbows and T-junctions, and
– the use of galvanized fittings with inherently rough internal surfaces.

In some regions of the circuit, pressure drops exceeded 20 bar, which was especially problematic during cold weather operation using ISO VG 46 hydraulic oil with elevated viscosity. Furthermore, friction-induced heating within the hoses led to localized reductions in oil viscosity, which slightly altered pressure readings and introduced variations between measured and simulated data. Despite these challenges, the close agreement between simulation results and physical measurements, particularly during bypass testing, validates the accuracy of the modeling approach. Notably, increasing the internal line diameter resulted in substantial reductions in peak pressure – from 92 bar to 26 bar for the 20 cc pump, and from 53 bar to 18 bar for the 16 cc pump. These outcomes underscore the effectiveness of diameter optimization as a means to enhance energy efficiency without requiring complete hardware replacement. Lastly, achieving reliable simulation fidelity depended heavily on incorporating precise component-level parameters into the model. These included bend radius, pipe roughness, and cross-sectional geometry of T-junctions, all of which had measurable influence on flow resistance and pressure behavior.

Conclusions

This research provides a compelling case for combining physical experimentation with simulation-based analysis to reveal and address hidden energy losses in mobile hydraulic systems. Through a targeted design improvement. Specifically the enlargement of pipe diameters and reduction of localized restrictions, system-level energy efficiency was improved significantly. The 7 kW of recovered hydraulic energy represents approximately 13% of the total power supplied by the engine-driven pumps. Notably, these gains were accomplished without replacing any mechanical components, thereby minimizing costs and operational downtime. The use of MATLAB SIMULINK proved invaluable in exploring hypothetical scenarios and performing sensitivity analyses to validate design decisions. This approach paves the way for future implementation of digital twin methodologies in fluid power systems. By integrating real-time sensor feedback, transient flow modeling, and iterative simulation, engineers can proactively identify and mitigate inefficiencies. Ultimately, this strategy fosters the creation of adaptive, resilient, and energy-conscious hydraulic architectures for next-generation mobile machinery.

Acknowledgment

We would like to acknowledge the funding provided by R&D Center of EYS Company and for providing the testing facilities for this case study. We would also like to acknowledge the Department of Mechanical Engineering at Aydin Adnan University for their support.

References

[1] Liu, J., *et al.*, Sensor Technologies for Hydraulic Valve and System Performance Monitoring: Challenges and Perspectives, *Adv. Sens. Res., 3* (2024), 3, 2300130
[2] Mahato, A. C., Ghoshal, S. K., Energy-Saving Strategies on Power Hydraulic System: An Overview. *Proc. Inst. Mech. Eng. Part J. Syst. Control Eng., 235* (2021), 2, 147169
[3] Eriksson, B., Palmberg, J.-O., Individual Metering Fluid Power Systems: Challenges and Opportunities. *Proc. Inst. Mech. Eng. Part J. Syst. Control Eng., 225* (2011), 2, 196211
[4] White, F. M., *Fluid Mechanics*, McGraw-Hill Series in Mechanical Engineering, 7. ed., McGraw-Hill: New York, USA, 2011
[5] *** ISO 4413:2010 Hydraulic Fluid Power — General Rules and Safety Requirements for Systems and Their Components; 2025
[6] Parr, E. A. *Hydraulics and Pneumatics: A Technician's and Engineer's Guide*, Butterworth Heinemann: Jordan Hill, Oxford, 1991
[7] Valdes, J. R., *et al.*, A Methodology for the Parametric Modelling of the Flow Coefficients and Flow Rate in Hydraulic Valves, *Energy Convers. Manag., 88* (2014), Dec., pp. 598-611
[8] De Moraes, M. S., *et al.*, Experimental Quantification of the Head Loss Coefficient K for Fittings and Semi-Industrial Pipe Cross Section Solid Concentration Profile in Pneumatic Conveying of Polypropylene Pellets in Dilute Phase, *Powder Technol., 310* (2017), Apr., pp. 250-263
[9] Li, D., *et al.*, Investigation Methods for Analysis of Transient Phenomena Concerning Design and Operation of Hydraulic-Machine Systems - A Review, *Renew. Sustain. Energy Rev., 101* (2019), Mar., pp. 26-46
[10] Liu, H., *et al.*, Research on Energy Consumption of Injection Molding Machine Driven by Five Different Types of Electro-Hydraulic Power Units, *J. Clean. Prod. 242* (2020), 118355
[11] Chuang, G. Y., Ferng, Y. M., Investigating Effects of Injection Angles and Velocity Ratios on Thermal-Hydraulic Behavior and Thermal Striping in a T-Junction, *Int. J. Therm. Sci. 126* (2018), Apr., pp. 74-81
[12] Yan, X., *et al.*, An Energy-Saving Method to Reduce the Installed Power of Hydraulic Press Machines. *J. Clean. Prod. 233* (2019), Oct., pp. 538-545
[13] Zhang, J., *et al.*, Delay Analysis and the Control of Electro-Hydrostatic Actuators, *Appl. Sci., 12* (2022), 6, 3089
[14] Stosiak, M. The Modelling of Hydraulic Distributor Slide–Sleeve Interaction, *Arch. Civ. Mech. Eng.* (2012), Apr., pp. 192-197

Paper submitted: November 14, 2024
Paper revised: February 14, 2025
Paper accepted: May 8, 2025